



OPEN ACCESS

EDITED BY

Matthijs Ruitenbeek,
Dow Benelux, Netherlands

REVIEWED BY

Giorgia De Guido,
Polytechnic University of Milan, Italy
Jingxiu Xie,
University of Groningen, Netherlands

*CORRESPONDENCE

J. Boon,
✉ jurriaan.boon@tno.nl
I. Tyraskis,
✉ jtyraskis@gmail.com

RECEIVED 01 November 2024

ACCEPTED 03 January 2025

PUBLISHED 31 January 2025

CITATION

Tyraskis I, Capa A, Skorikova G, Sluijter SN and Boon J (2025) Performance optimization of sorption-enhanced DME synthesis (SEDMES) from captured CO₂ and renewable hydrogen. *Front. Chem. Eng.* 7:1521374. doi: 10.3389/fceng.2025.1521374

COPYRIGHT

© 2025 Tyraskis, Capa, Skorikova, Sluijter and Boon. This is an open-access article distributed under the terms of the [Creative Commons Attribution License \(CC BY\)](https://creativecommons.org/licenses/by/4.0/). The use, distribution or reproduction in other forums is permitted, provided the original author(s) and the copyright owner(s) are credited and that the original publication in this journal is cited, in accordance with accepted academic practice. No use, distribution or reproduction is permitted which does not comply with these terms.

Performance optimization of sorption-enhanced DME synthesis (SEDMES) from captured CO₂ and renewable hydrogen

I. Tyraskis*, A. Capa, G. Skorikova, S. N. Sluijter and J. Boon*

TNO Energy and Materials Transition, Petten, Netherlands

Sorption-enhanced dimethyl ether synthesis (SEDMES) is a powerful technology to produce dimethyl ether (DME) from captured CO₂ and renewable H₂. *In situ* water by-product removal by zeolites shifts the thermodynamic equilibrium of the reaction towards product formation. Sorption enhancement proved to provide a single-pass CO₂ conversion above 90%. This work presents a modelling study of the SEDMES process to optimize its performance under varying conditions. A universal cycle was designed to fulfil the requirement of continuous DME production as well as feed and purge flows. The cycle design is based on a state-of-the-art pilot plant commissioned by TNO in 2023, located in Petten, The Netherlands. Multiple Pareto fronts were generated to express the trade-offs between DME productivity and carbon selectivity in the SEDMES process for the first time. The impact of such process parameters as operating pressure, cycle duration, amount of inert gases, tube geometry and feed flow rate was analysed. A general trend of increased carbon selectivity and productivity at higher pressure was observed and analyzed under relevant cycle durations. However, this enhanced performance comes with the negative side effect of higher DME loss associated at elevated pressure operation. The SEDMES process proved to be tolerant to high concentrations of inert gases such as N₂, reducing the need for extensive pretreatment steps. A lower feed flow rate was found to positively impact carbon selectivity to DME, which is promising for operation under intermittent conditions. Finally, even a minor increase in tube diameter reduced the Gas Hourly Space Velocity (GHSV), enhancing DME selectivity in a manner comparable to the effect of lower feed flow rates. Maximum productivity increases from 2.2 kg/h with 50.2% DME selectivity at 20 bar to 3.6 kg/h with 88.5% DME selectivity at 50 bar. The optimal cycle duration for these points also increased from 113 to 233 min, respectively.

KEYWORDS

dimethyl ether, carbon/CO₂ utilization, modelling, sorption enhanced, pressure-swing adsorption (PSA)

Abbreviations: SEDMES, Sorption-enhanced dimethyl ether synthesis; DME, Dimethyl ether; GHSV, Gas hourly space velocity; PSA, Pressure-swing adsorption; CCS, Carbon Capture and Storage; CCU, Carbon Capture and Utilization; GHG, Greenhouse Gases; LPG, Liquefied petroleum gas; TRL, Technology readiness levels; TPSA, Temperature and Pressure Swing Adsorption; PEM, Proton Exchange Membrane; TNO, Netherlands Organisation for Applied Scientific Research; LTA, Linde Type A; ADS, Adsorption step; BD, Blowdown step; P, Purge step; REP, Re-pressurization step; S (DME), Selectivity towards dimethyl ether; KPI, Key performance indicator; r-WGS, Reverse water gas shift.

1 Introduction

Climate change is one of the most important challenges our society faces nowadays. To combat climate change, industrial processes, products and feedstock need to become climate neutral, and industrial cycles have to be closed by 2050 which is the heart of the European Green deal (European Commission, 2019). In order to achieve those targets, the Paris Agreement (Delbeke et al., 2019) claimed that the temperature rise should be kept at no more than 1.5°C meaning that the emissions need to be limited between 250 and 450 GtCO₂ (van Vuuren et al., 2017). To achieve this, the European Climate law (European Commission, 2021) established that the emissions must be reduced by at least 55% by 2030 compared to 1990 levels in order to achieve the climate-neutrality by 2050. To reduce CO₂ emissions, future perspectives will not only concern development and optimization of Carbon Capture and Storage (CCS) systems, but mainly conception and demonstration of new efficient strategies for carbon dioxide capture and utilization (CCU) (Catizzone et al., 2021). Through CO₂ utilization, captured CO₂ can be utilized as the raw material in manufacturing high value chemical products such as polycarbonate copolymerization, fuel through methanation, methanol as well as formic acid through hydrogenation, DME through dehydration of methanol and other chemicals and reagents.

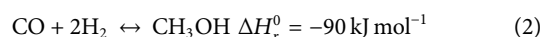
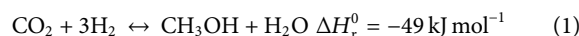
Among the CO₂ utilization methods, one of the most attractive routes for large-scale valorisation is the production of DME using CO₂ (Catizzone et al., 2021; Jia and Yin, 2024; Merkouri et al., 2022; Catizzone et al., 2017). Dimethyl ether, is the simplest ether and the dehydrated form of methanol. DME has a higher calorific value than methanol, and therefore higher amount of energy can be generated during the combustion process (Jia and Yin, 2024). At the same time it does not contain carbon-carbon bonds and thus, lower CO and Greenhouse Gases (GHG) emissions after burning can be achieved as well as very low NO_x and soot in the exhaust gases (Jia and Yin, 2024; Liuzzi et al., 2020). DME is well-suited for deployment as fuel in domestic applications replacing liquified petroleum gas (LPG), in compression ignition engines (100% DME), in spark ignition engines (30%DME/70%LPG), and in power generation. The global market for DME (dimethyl ether) has traditionally focused on its role as a chemical feedstock, used in producing, i.e., dimethyl sulfate, acetic acid, and as an aerosol propellant, solvent, refrigerant, and antifreeze. Meanwhile, the growing role of renewable DME as a drop-in fuel is expanding the market segments towards off-grid applications where it can be blended with LPG, and as a heavy-duty fuel that reduces soot emissions in diesel engines (van Kampen et al., 2023; Peinado et al., 2024). It is also considered a proposing platform chemical for producing olefines for plastics and jet fuel (Azizi et al., 2014a). Therefore, in recent years, interest in the conversion of carbon/CO₂ into DME has increased considerably. It has been reported in the literature that the production of DME from CO₂ via hydrogenation is at TRL 2-3 with a CO₂ utilization potential of 7.65 MtCO₂/year (Nimmas et al., 2024). On the other hand, DME can be produced from syngas as well, and the syngas route is already at a commercial stage (Altinsoy and Avci, 2024).

As reported in the literature, indirect DME production is a two-step process (Jia and Yin, 2024; Van Kampen et al., 2020a; Azizi et al., 2014a). First, intermediate methanol is synthesised from syngas or CO₂ (Equations 1, 2), followed by the dehydration of

methanol to DME (Equation 4) in a separate reactor. This process is well-established, both commercially and scientifically (Peinado et al., 2024), but as this system is thermodynamically limited, results in limited yield, extensive separations and large recycles. Therefore, in recent years, a lot of effort has been devoted to research on direct DME production in a single-step process (Equations 5, 6). The direct DME route benefits from the continuous conversion of one intermediate (MeOH) which shifts equilibrium towards DME production allowing for a simpler operation (Peinado et al., 2024; Saravanan et al., 2017; Dadgar et al., 2016).

Another enhancement can be done to the direct DME synthesis, which is the *in situ* H₂O removal. The *in situ* steam adsorption has been studied for different reactions such as reverse water-gas shift, the Claus process, the Sabatier process among others (Elsner et al., 2002; Elsner et al., 2003; Schmidt-Traub and Górák, 2006; Walspurger et al., 2014; Borgschulte et al., 2013). In this regard, SEDMES is a novel process for the production of DME, in which water is removed *in situ* through the use of a solid adsorbent, shifting the equilibrium to the product side based on Le Chatelier's principle (Equation 6). As reported in the literature one of the challenges in conventional processes is to improve the stability of the catalysts, because those materials can be easily deactivated through sintering and poisoning by water (Jia and Yin, 2024; Mohamud et al., 2023). The *in situ* removal of steam in the SEDMES concept, has been shown to enhance catalysts lifetime and boost process efficiency, specifically in the case of diluted CO₂-rich gas streams (Skorikova et al., 2020). The complete set of reactions is as follows Equations 1–6:

Methanol synthesis



Water gas shift



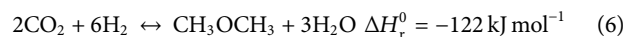
Methanol dehydration



Direct DME synthesis (from CO)



Sorption Enhanced direct DME synthesis (from CO₂)



The effect of water removal on liquid phase DME synthesis from syngas was studied by Kim et al. who proved that the removal of water was efficient in maintaining a high catalytic activity and stability of the Cu/ZnO/Al₂O₃ and γ-Al₂O₃ (Kim et al., 2001). Iluta et al. showed the potential of the *in situ* H₂O removal for the first time by the modelling of a multiscale reactor (Iluta et al., 2011). The SEDMES concept has been evaluated by modelling (Iluta et al., 2011; Boon et al., 2017; Guffanti et al., 2021a) and it has also been demonstrated by experimental proof-of-concept showing that both, the DME yield and also the DME selectivity are improved over conventional processes achieving DME yields of at least 80% with a reduced amount of CO₂ in the product stream (Liuzzi et al., 2020; Altinsoy and Avci, 2024; Boon et al., 2017; Kampen et al., 2018; Van

TABLE 1 Reactor model equations.

Continuity/overall mass balance	$\frac{\partial \rho}{\partial t} = -\frac{\partial \rho v}{\partial z} - \frac{1 - \varepsilon_b}{\varepsilon_b} a_p \sum M_i N_i \quad (\text{A})$
Momentum balance	$\frac{\partial \rho v}{\partial t} = -\frac{\partial \rho v^2}{\partial z} - \frac{\partial P}{\partial z} - G \frac{\rho u u}{d_p} \quad (\text{B})$
Species mass balance	$\frac{\partial \rho \omega_i}{\partial t} = -\frac{\partial \rho v \omega_i}{\partial z} + \frac{\partial}{\partial z} (D_z \rho \frac{\partial \omega_i}{\partial z}) - \frac{1 - \varepsilon_b}{\varepsilon_b} a_p M_i N_i \quad (\text{C})$
Overall energy balance	$(\varepsilon_b \rho C_p + (1 - \varepsilon_b) \rho_p C_{p,p}) \frac{\partial T}{\partial t} = -\rho C_p v \frac{\partial T}{\partial z} + \frac{\partial}{\partial z} (\lambda \frac{\partial T}{\partial z}) + \frac{4U(T_w - T)}{d_r} + (1 - \varepsilon_b) \rho_p \left(\sum -\Delta H_{r,i} r_i + \sum -\Delta H_{ads,i} \frac{\partial q_i}{\partial t} \right) \quad (\text{D})$
Equation of state	$PM = \rho RT \quad (\text{E})$

Kampen et al., 2020b; Van Kampen et al., 2021). The regeneration of the Adsorbent is one of the key parameters for the optimization of SEDMES process. In a first experimental study it was concluded that a combination of temperature and pressure swing regeneration (TPSA) could result in the best performance regarding the DME yield and the CO₂ conversion (Van Kampen et al., 2020a). However, in a more recent study in which SEDMES is experimentally tested under industrially relevant conditions, similar conversion and selectivity were obtained with PSA in comparison with the previous TPSA. Since the faster pressure swing regeneration increased the DME productivity by a factor of four, the preferred operation mode of SEDMES is PSA (Van Kampen et al., 2020b; Van Kampen et al., 2021). This was recently confirmed in a modelling study (Van Kampen et al., 2020a). The SEDMES concept using PSA operation has been recently validated for the first time in the open literature on a multi-column test-rig under industrially relevant conditions demonstrating the continuous DME production by sorption-enhancement, for which up to 95% carbon yield was observed (van Kampen et al., 2023). The SEDMES Power-to-X technology has the potential to reduce life-cycle GHG emissions of transport fuel by up to 91% compared to fossil fuels if the electricity used for both CO₂ capture and DME production (including H₂ production) is derived from offshore wind and the heat required is waste heat from, for example, municipal waste incineration (Styring et al., 2022). Additionally, the production cost of DME using SEDMES technology was estimated to be around 1.3 €/kg for a relatively small-scale production plant 23 kt/year when using H₂ produced by a PEM electrolyzer and captured CO₂ (Skorikova et al., 2020).

In SEDMES, the chemical reaction and adsorption are combined since it is a reactive adsorption process and as a typical PSA process it is operated in cycles between reactive adsorption and adsorbent regeneration (Skorikova et al., 2020). The practical issue of sorption enhanced reaction processes is the discontinuous operation of the reactor because at the equilibrium of the adsorbent the separation effect is lost. Therefore, a periodic regeneration of the adsorbent is needed (Iliuta et al., 2011). In this work, the cycle design that operates at the largest dedicated SEDMES installation built at TNO Petten, Netherlands, for the continuous DME production is used as reference for the modelling. More details about the cycle design are explained in the methodology section.

The SEDMES pilot plant at Petten has been designed, built and commissioned until 2023 and uses commercially available catalysts and adsorbents. The main development steps are related to process optimisation and scaling-up (Boon, 2023). In this work the effect of the pressure, cycle duration, feed flow and some other insights about the SEDMES performance are evaluated to show optimization strategies using a previously developed one-dimensional cyclic dynamic model (Van Kampen et al., 2020a). Additionally, this paper is building knowledge on the SEDMES optimization by reporting for the first time the pareto plots obtained for the case study in which DME is produced from captured CO₂ and renewable H₂. In the pareto plots, a trade-off between C-selectivity towards DME and DME productivity can be observed and will be part of the main discussion in this work.

2 Methodology

A one-dimensional pseudo-homogeneous dynamic reactor model was previously developed in Matlab, verified and validated (Van Kampen et al., 2020a). For the description of the fluid flow and mass transfer, the 1D non-steady differential mass and momentum balances are solved. The total mass, momentum, component and overall energy balances are given in Table 1. Reaction kinetics were determined for the catalysts by fitting the parameters in the models of Graaf et al. (1988) and Bercic and Levec. (1992) for the methanol synthesis and methanol dehydration respectively, shown in Table 2 (Boon et al., 2019; Graaf et al., 1988; Bercic and Levec, 1992). The steam adsorption isotherm of the LTA zeolite adsorbent was determined under the high pressure and temperature working conditions of the SEDMES process. A Sips isotherm best describes the experimental data, in accordance with the available literature at lower temperature and pressure conditions (Kim et al., 2016; Gabruš et al., 2015). Full details of the different aspects of the model can be found in our previous work (Van Kampen et al., 2020a).

The SEDMES pilot plant commissioned at Petten, The Netherlands, is shown in Figure 1A). Copper-based methanol synthesis and gamma alumina dehydration catalysts are present in the reactors, as is a zeolite 3A for *in situ* water removal. This pilot

TABLE 2 Reaction rate equations.

Methanol synthesis from CO (Graaf et al., 1988)	$r_{CH_3OH,1} = \frac{k_1 K_{CO} [\varphi_{CO} \varphi_{H_2}^{3/2} - \varphi_{CH_3OH} / (\varphi_{H_2}^{1/2} K_{p1})]}{(1 + K_{CO} \varphi_{CO} + K_{CO_2} \varphi_{CO_2}) [\varphi_{H_2}^{1/2} + (K_{H_2O} / K_{H_2}^{1/2}) \varphi_{H_2O}]}$ (F)
Water gas shift (Graaf et al., 1988)	$r_{CO} = \frac{k_2 K_{CO_2} [\varphi_{CO_2} \varphi_{H_2} - \varphi_{H_2O} \varphi_{CO} / K_{p2}]}{(1 + K_{CO} \varphi_{CO} + K_{CO_2} \varphi_{CO_2}) [\varphi_{H_2}^{1/2} + (K_{H_2O} / K_{H_2}^{1/2}) \varphi_{H_2O}]}$ (G)
Methanol synthesis from CO ₂ (Graaf et al., 1988)	$r_{CH_3OH,2} = \frac{k_3 K_{CO_2} [\varphi_{CO_2} \varphi_{H_2}^{3/2} - \varphi_{CH_3OH} \varphi_{H_2O} / (\varphi_{H_2}^{3/2} K_{p3})]}{(1 + K_{CO} \varphi_{CO} + K_{CO_2} \varphi_{CO_2}) [\varphi_{H_2}^{1/2} + (K_{H_2O} / K_{H_2}^{1/2}) \varphi_{H_2O}]}$ (H)
Methanol dehydration (Bercic and Levec, 1992)	$r_{DME} = \frac{k_4 K_{CH_3OH}^2 [C_{CH_3OH}^2 - C_{H_2O} C_{DME} / K_{p4}]}{[1 + 2(K_{CH_3OH} C_{CH_3OH})^{1/2} + K_{H_2O} C_{H_2O}]^4}$ (I)

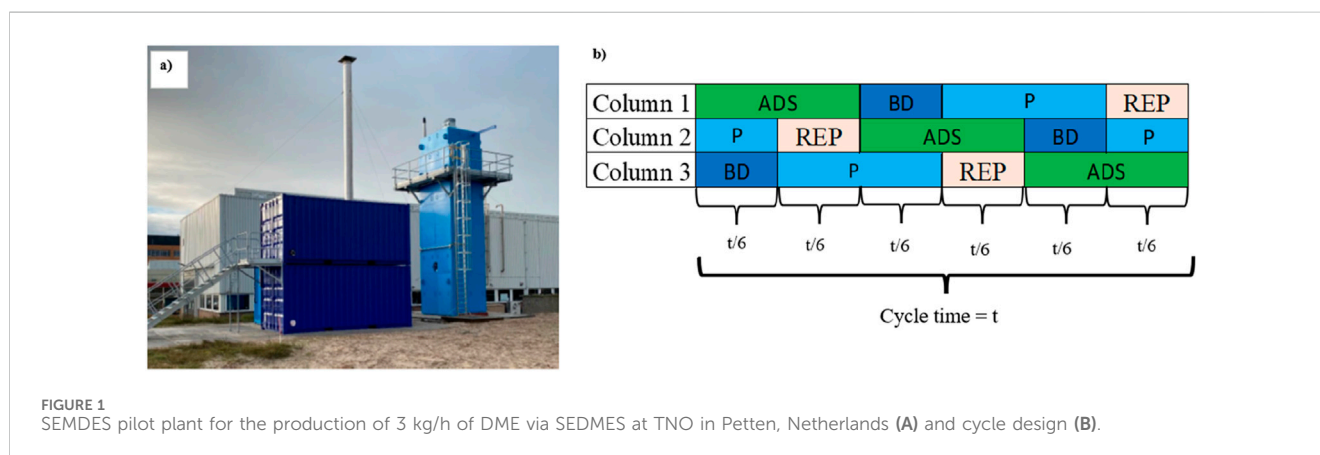


FIGURE 1 SEMDES pilot plant for the production of 3 kg/h of DME via SEDMES at TNO in Petten, Netherlands (A) and cycle design (B).

is equipped with three reactor columns, working as a shell and tubes heat exchanger reactor. Inside each reactor there are 19 tubes of 7.6 m height and 36.6 mm internal diameter. Hot oil circulates between the tubes as heating medium.

The three reactors are producing DME continuously going each of them through the various steps of the cycle explained in Figure 1B. Each cycle has four consecutive steps: adsorption (ADS) is the step in which DME is produced with *in situ* water removal under the selected pressure; blowdown (BD) is the depressurization of the system in order to prepare the system for the pressure swing regeneration; purge (P) is the step in which the water adsorbent is regenerated using H₂ as purge gas at ambient pressure and finally, re-pressurization (REP) is when the column is repressurised in order to be ready for the next ADS step. H₂ is used for the re-pressurization step unless otherwise specified. In this work, the specific three-column cycle design shown in Figure 1B), has been used and is kept the same for all the simulations.

The case analysed in this study is derived from the utilisation of captured CO₂ from the oil and gas sector and renewable hydrogen. The CO₂ capture unit is out of the scope of this study. Hydrogen is added in order to obtain M-module = 2 (Equation 7), meaning a feed that contains 12 wt% of H₂ and 88 wt% CO₂.

$$M - \text{module} = \frac{H_2 (\text{mol. \%}) - CO_2 (\text{mol. \%})}{CO_2 (\text{mol. \%})} \quad (7)$$

The maximum feasible flow of the pilot has been assumed for the adsorption, purge and re-pressurization steps (20,

25 and 34 Nm³/h respectively) unless otherwise specified. As described in literature (Van Kampen et al., 2020a), a typical window for the SEDMES process includes adsorption temperatures between 250°C and 275°C and pressures of 20 bar or more (Van Kampen et al., 2020a). In order to find the region of optimal operation for this case study at different pressures, different cycle times were simulated for six different pressures (20, 25, 30, 35, 40 and 50 bar), whereas the temperature has been fixed to 250°C. The performance was evaluated by analyzing the pareto plots showing the DME productivity and selectivity at the different operating pressures. By changing the duration of each step of the cycle while keeping the ratio of step time over total cycle time constant to ensure continuous operation, the optimum is found.

The main key performance indicators studied in this work are the SEDMES pilot plant DME productivity and the carbon selectivity towards DME (S (DME)). These KPIs are calculated using Equations 8, 9 respectively. The carbon selectivity towards DME is calculated as molar concentration-based selectivity for each of the carbon containing species *y* (i).

$$DME \text{ productivity } (kg \text{ DME}/h) = \frac{DME \text{ production } (kg)}{\text{Cycle time } (h)} \quad (8)$$

$$S(DME) = \frac{2y(DME)}{y(CO) + y(CO_2) + y(MeOH) + 2y(DME)} \quad (9)$$

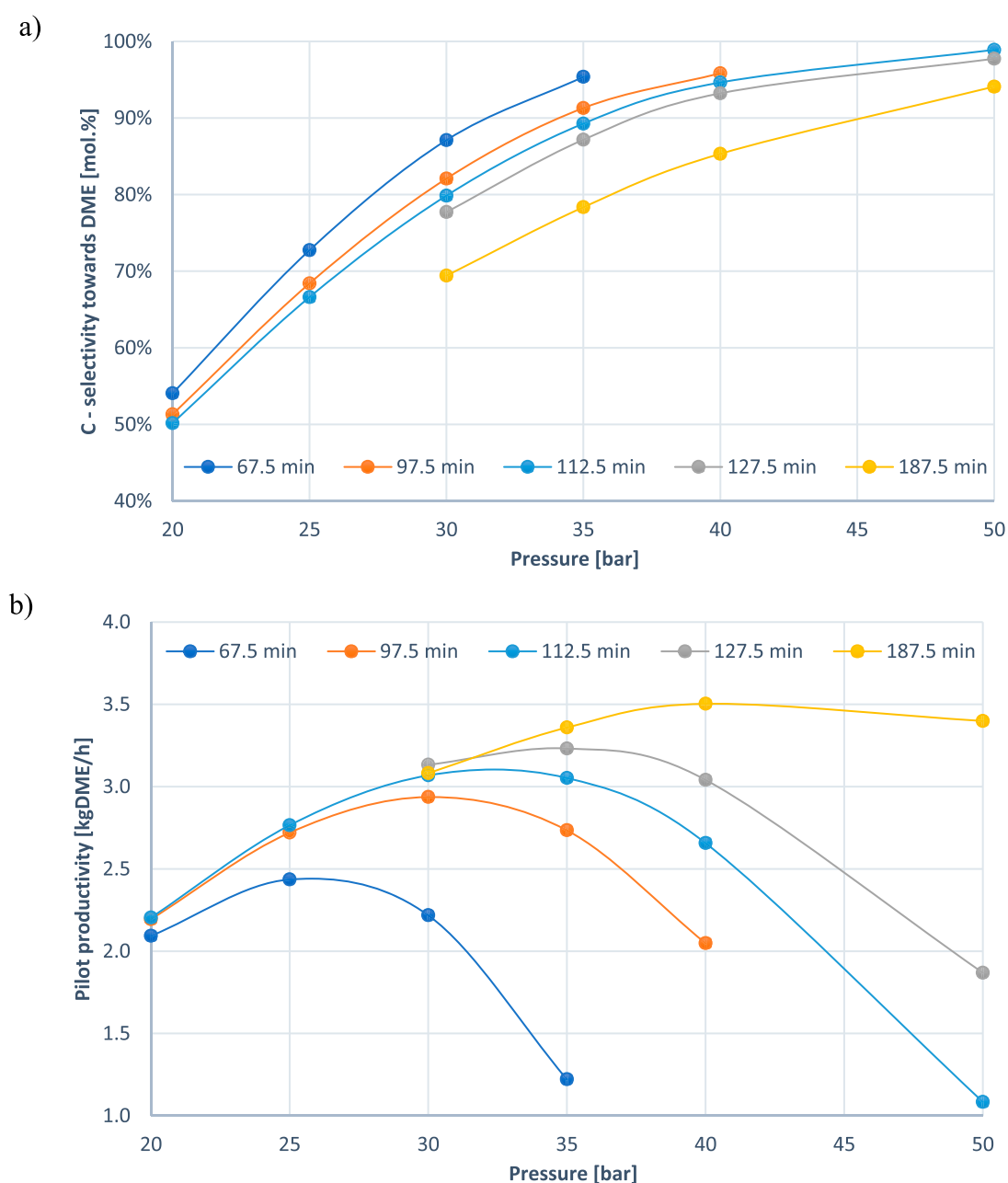


FIGURE 2 Effect of pressure on the carbon selectivity towards DME (A) and the pilot DME productivity (B). Every line represents a different cycle duration.

3 Results and discussion

3.1 DME selectivity and productivity

3.1.1 Importance of pressure in SEDMES optimization

The choice of total pressure in the adsorption step has three main implications for the performance of the SEDMES cycle (European Commission, 2019): the thermodynamic equilibrium changes (Delbeke et al., 2019), increase in the steam partial pressure increases the equilibrium amount of water adsorbed, and (van Vuuren et al., 2017) more gas is required for the re-

pressurization of the column (Van Kampen et al., 2020a). Even though previous studies have noted DME production at pressures up to 70 bar (De Falco et al., 2017), and demonstrated higher conversion at elevated pressures (Van Kampen et al., 2020a), optimizing the process performance at each pressure level, and quantification of the potential benefit is missing.

Figure 2A, B illustrates the impact of pressure on both carbon selectivity towards DME and pilot DME productivity, respectively. The data reveal that increasing pressure enhances DME selectivity. It should be noticed that in all the simulations of this work H_2 is the re-pressurization gas. A similar trend was shown in the literature before when using syngas for the re-pressurization. For syngas

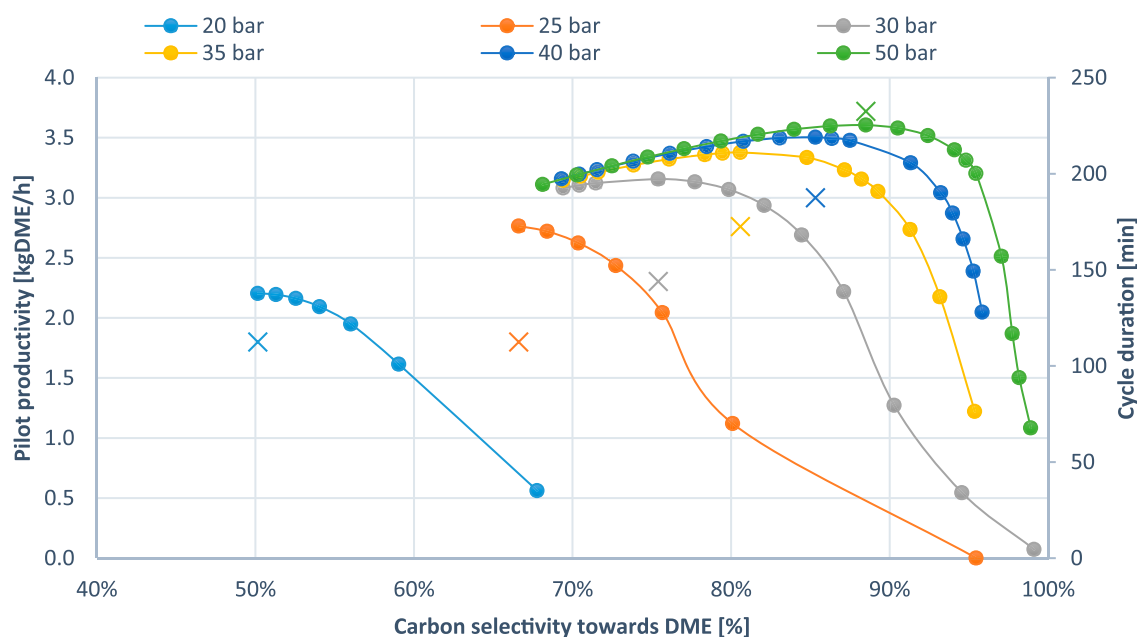


FIGURE 3
Pareto plot showing the SEDMES productivity-selectivity trade-off as a function of the pressure. The "X" symbol indicates the cycle duration for the maximum productivity (displayed on the secondary y-axis). The cycle duration increases as the curve progresses from right to left, towards lower DME selectivities.

re-pressurization it has been discussed that during the re-pressurization more syngas is fed at higher pressures causing an increase in the GHSV. Although an increased GHSV results in a lower conversion towards DME, the positive effect of the pressure on reaction and adsorption is more pronounced than the small increase in GHSV (Van Kampen et al., 2020a). A similar trend is happening when doing re-pressurization with H_2 (Figure 2A) where it can be additionally observed that the selectivity decreases when increasing the cycle duration. Conversely, the relationship between pressure and pilot productivity (Figure 2B) shows that productivity increases with pressure up to a certain point, after which it sharply declines, especially with shorter cycle times, showing a clear maximum in terms of productivity for a specific cycle duration.

As cycle duration increases, the amount of feedstock treated increases, and water accumulates in the system unless efficiently removed by adsorption. Gradual adsorbent saturation leads to insufficient removal of water which can inhibit the desired reactions and promote the side reaction of reverse water-gas shift (r-WGS), which diverts reactants away from methanol and DME formation (Liuzzi et al., 2020). Over time, selectivity towards DME is reduced, even with active water adsorption. At a certain point, the system reaches an optimal balance, where water adsorption effectively shifts the equilibrium, maximizing productivity. However, as the cycle duration continues to increase beyond this peak, the system's ability to maintain high selectivity diminishes. This decline is attributed to the production of by-products and the reduced efficiency of water adsorption over time. The peak in productivity occurs when water adsorption still effectively shifts the equilibrium, but before selectivity loss from side reactions becomes too significant.

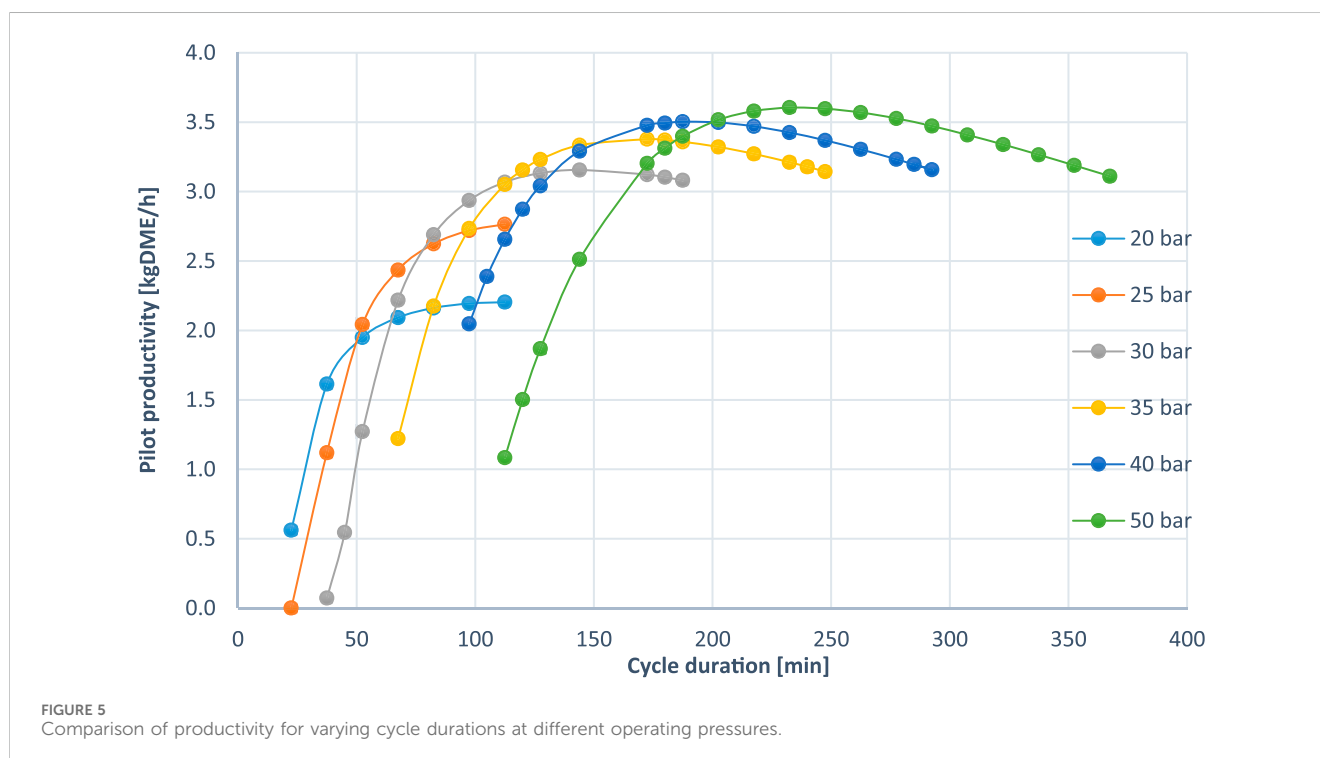
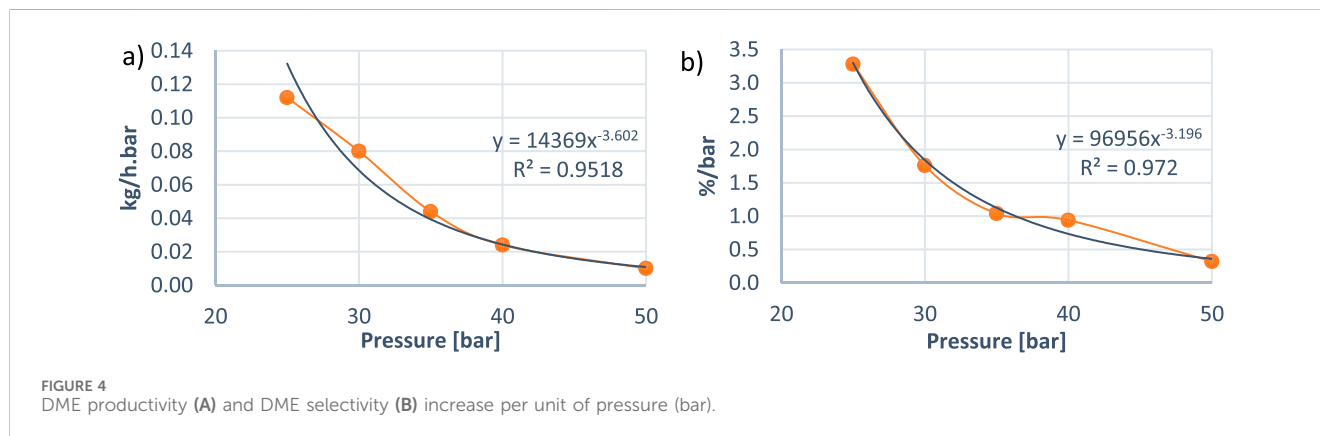
Given this behaviour, a trade-off between selectivity and productivity can be identified by creating a pareto plot (Figure 3). Examining the plot of productivity versus carbon selectivity to DME clarifies the performance advantages associated with operating at higher pressures, as it displays the productivity peaks across all simulated cycle durations for varying pressures from 20 to 50 bar. The graph consistently leads to two conclusions across all simulations and cases:

1. Higher operating pressures show higher productivity peaks.
2. Higher pressures show productivity peaks at larger cycle durations.

Operating at 50 bar, the highest pressure evaluated, delivers the most significant advantages in both productivity and DME selectivity, achieving 3.6 kg/h and approximately 90% DME selectivity. The positive effect on the performance of the SEDMES process at elevated pressures was reported in the literature before reporting DME selectivity up to 76.7% at 50 bar operating pressure (Van Kampen et al., 2020a). In this work, it is observed from the pareto plots that optimizing the cycle time, the selectivity can be further increased showing for the first time values as high as 88.5% at 50 bar operating pressure. Nonetheless, the incremental gains in DME productivity and selectivity become less pronounced as pressure increases, as evidenced by the detailed values for the productivity peaks presented in Table 3. Additionally, it is apparent, particularly in simulations conducted at higher pressures, that an increase in pressure results in the highest gains in productivity for simulations with the highest selectivity (shorter duration). This happens because shorter cycle durations, where methanol and DME

TABLE 3 Maximum productivity and selectivity for each analysed pressure.

Pressure (bar)	20	25	30	35	40	50
Max productivity (kg/h)	2.20	2.76	3.16	3.38	3.50	3.60
DME selectivity at maximum productivity	50.2%	66.6%	75.4%	80.6%	85.3%	88.5%



formation from CO/CO₂, dominate over side reactions, take full advantage of the pressure-driven equilibrium shift, maximizing the production of DME before side reactions, such as r-WGS, can become prominent.

The effect of increasing pressure on system performance was quantified by analyzing the maximum productivity points at various operating pressures, providing a consistent reference for comparison across different conditions. As illustrated in

Figure 4A, the productivity gain per unit pressure decreases at a diminishing rate with rising pressure. A similar trend is observed in Figure 4B for selectivity per unit pressure, with one notable exception: a sharp decline in the rate of selectivity increase between 25 and 30 bar, followed by a stable rate from 35 to 40 bar. This anomaly may be mitigated by refining the selection of productivity peak points through smaller cycle duration increments in simulations. Comparing the rates of increase at lowest and highest pressures reveals that DME

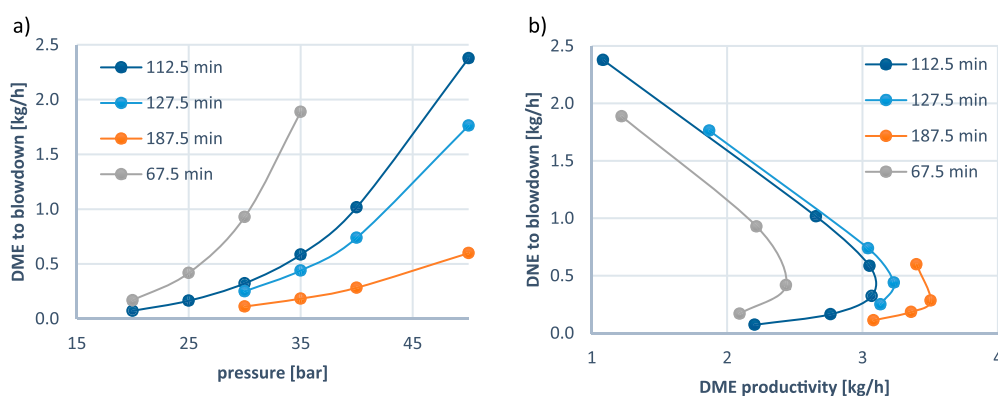


FIGURE 6

(A) Effect of the pressure on the DME losses during the blowdown step for different cycle durations. (B) Trade-off between DME productivity and DME loss to blowdown at increasing operating pressure for different cycle durations.

productivity increased by 0.11 kg/hbar and DME selectivity by 2.4%/bar between 20 and 25 bar, while the increments were only 0.03 kg/hbar and 0.4%/bar, respectively, between 40 and 50 bar. Overall, the results suggest that the rates of productivity and selectivity increase follow a power law relationship with pressure, where productivity is proportional to $x^{-3.6}$ and selectivity is proportional to $x^{-3.2}$.

3.1.2 Effect of cycle duration

As illustrated in Figure 3, an increase in pressure necessitates a longer cycle duration. This occurs because, while more water is being produced because of the higher DME productivity, this effect is more than offset by the increase in working capacity for water of the adsorbent at the higher pressure swing operation. The simulation results, plotted along various pressure curves as illustrated in Figure 5, reveal a peak in productivity at a specific cycle duration. However, extending the cycle duration consistently results in a decrease in selectivity. This trend aligns with the observations described in the previous chapter and is attributed to water hold-up and adsorbent saturation during prolonged operations, as previously explained.

Cycle duration is a critical parameter for optimizing the operation of the process, as it governs the interaction between the reactants, products, and adsorbent within the system without practical limitations in terms of the values it can take. For any given set of operating conditions, there exists an optimal cycle duration that maximizes productivity or achieves a desired selectivity. It is important to highlight, however, that cycle duration applies to all stages of the SEDMES process, not just the adsorption step. Prolonged cycle durations may result in unnecessarily extended blowdown, purge, or re-pressurization phases, which could introduce economic inefficiencies. Therefore, while cycle duration offers flexibility in process optimization, careful consideration must be given to its impact on the overall cycle to avoid excessive operational costs.

3.2 Other aspects of SEDMES optimization

3.2.1 Loss in blowdown

One point that it is important to consider in this cyclic process, is the amount of the targeted product (DME) that is lost during the

blowdown (depressurization step) which follows the adsorption step. This step of the process in which the pressure of the column is released is where there is the highest risk of product losses since some areas of the column could still contain DME. The effect of the pressure on the DME losses during the blowdown step is shown in Figure 6A for different cycle times. It can be observed that for a given cycle time, the higher the pressure, the higher the DME that is lost to the blowdown stream. Additionally, shorter cycles, are particularly susceptible to this effect, experiencing more significant DME losses with increasing pressure. A notable example is the 67.5-min cycle, where DME loss nearly doubles from 0.92 to 1.89 kg/h when the pressure increases from 30 to 35 bar.

Figure 6B further highlights the trade-off between DME productivity and DME loss to blowdown, identifying an optimal operating point for maximum productivity for each cycle duration. While higher pressures enhance DME productivity, they simultaneously escalate DME losses, eventually reaching a threshold beyond which further pressure increases become unfavorable. As a result, despite the improved productivity and selectivity at elevated pressures, these material losses may necessitate operating at lower pressures, longer cycle durations, or incorporating effective recycling strategies to optimize the process.

As indicated in literature, the blowdown stream could be recycled back to the feed of the adsorption step after undergoing re-pressurization and possibly drying (Van Kampen et al., 2020a). However, elimination of unnecessary purification and recycling steps could lead to relevant reduction in overall costs (van Kampen et al., 2019a), particularly when considering the already negative impact of operating at excessively high pressures. High pressure operation requires expensive equipment, higher operational costs due to increased demand for compression, and introduces additional complexities, such as the risk of coke formation (Dieterich et al., 2020). This creates a trade-off between the thermodynamic benefits and the associated capital and operational expenditures as described by Guffanti et al. 2021a. Therefore, while lower pressure operation might reduce the efficiency of the adsorption step, it could still lower the levelized cost of DME production. Incorporating such system

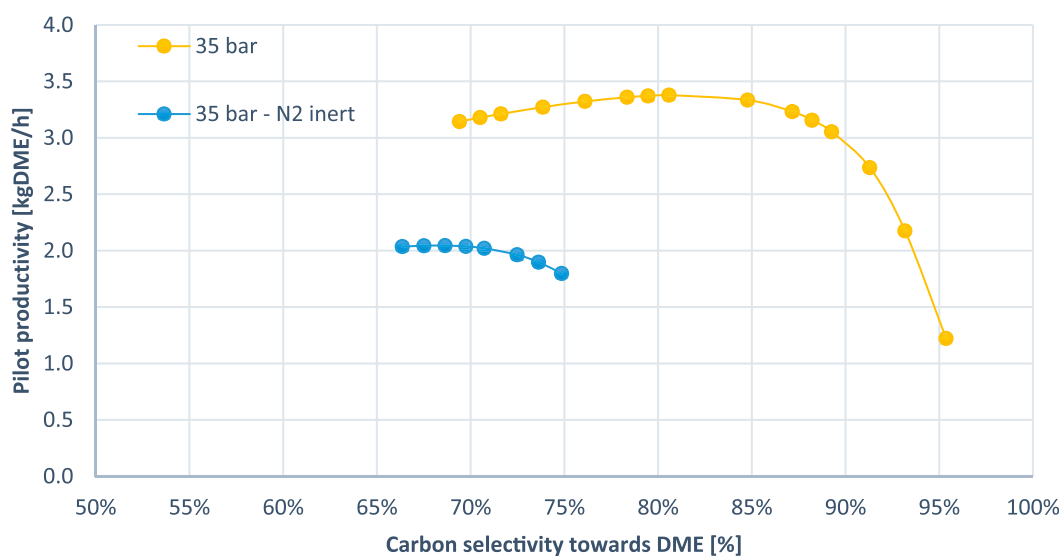


FIGURE 7 SEDMES operation with 50 wt% content of inert N_2 in the adsorption feed (blue line) and 0 wt% content of inert N_2 (yellow line).

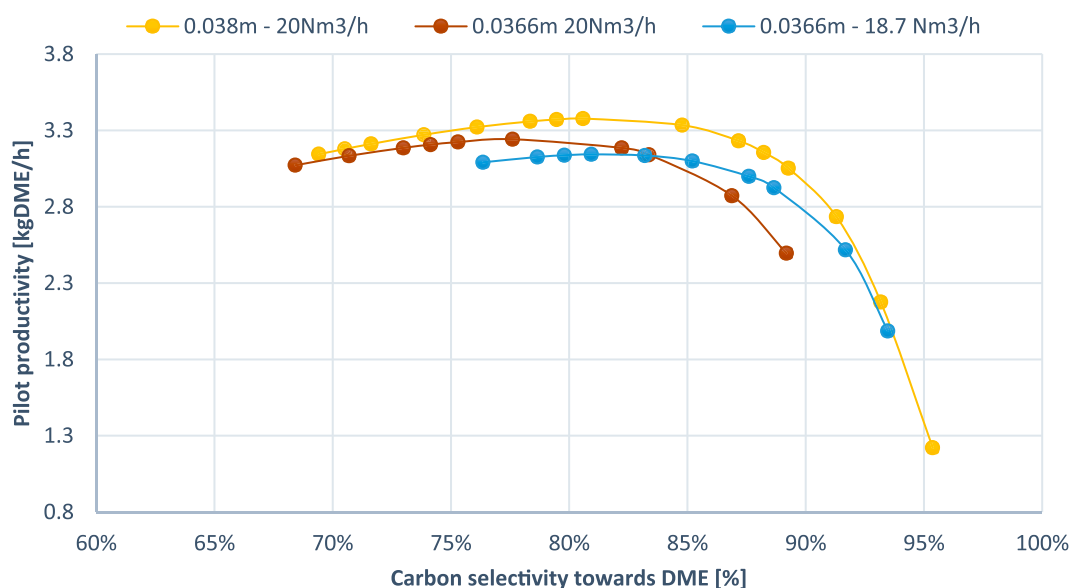


FIGURE 8 Comparison of DME productivity and selectivity for different tube diameters and feed flow rates at 35 bar.

optimization strategies into the existing techno-economic evaluation of the process (Skorikova et al., 2020) is a crucial future step to enhance the cost-competitiveness of SEDMES process.

3.2.2 Effect of inert gases in the feed

In this study, the raw CO_2 stream is enriched due to a carbon capture step. Potential elimination of this step or introduction of CO_2 from alternative industrial sources may result in the presence of inert gases such as N_2 and CH_4 , which are common in industrial off-gases. SEDMES has been experimentally proven to be able to operate under presence of inert. As presented by—Van Kampen et al.

(2020a), the experiments were conducted with up to 30 vol% N_2 , and it is expected that higher amounts are possible.

In order to evaluate the scenario of avoiding CO_2 pre-treatment, the case study was modelled with a feed composition containing 50 wt% N_2 (equivalent to 30 mol%) at 35 bar, maintaining an M-module of 2. Although inert gases, particularly N_2 , have been considered in previous studies (Van Kampen et al., 2020a; Kampen et al., 2018; Guffanti et al., 2021a) (Boon et al., 2017) (Guffanti et al., 2021c) (van Kampen et al., 2019a), SEDMES has not been examined at such high concentrations of inerts, nor has the impact on the performance of the process been quantified.

As shown in Figure 7, the inclusion of N_2 led to approximately a 40% reduction in DME productivity. This decline is attributed to the lower concentration of reactants, as the inert gas dilutes the feed stream. In addition, the range of DME selectivity near the maximum productivity point decreased significantly by about 20%. This could be due to the reduced contact between reactants and the catalyst, as the inert gas occupies space within the reactor, inhibiting effective mass transfer.

Despite the lower performance compared to a purified CO_2 feed, operation under these conditions remains technically feasible. This indicates that pre-treatment of the feed gas is not strictly necessary, even with an inert content of up to 30 mol%. Although the presence of inerts compromises process performance, this drawback could be balanced by the elimination of costly and energy-intensive pre-treatment steps. Future research should focus on the effects of various inert gases and specific industrial scenarios to further optimize process conditions and improve overall efficiency.

3.2.3 Effect of tube geometry

Lastly, the impact of tube diameter of the multi-tubular SEDMES reactor was assessed at 35 bar showing the pareto plot for carbon selectivity towards DME against DME productivity for two different tube diameters (0.038 m and 0.0366 m). The effect of tube diameter was studied by Guffanti et al. (2021a) before. In their study they considered tubes with internal diameters equal to 25.6, 38 and 46.6 mm. From all those cases, the 38 mm tube is the closest to the SEDMES pilot plant referred before which has a tube diameter of 36.6 mm. In this section, we are comparing the pareto plots for these two diameters (38 and 36.6 mm) aiming to develop more insights regarding the process optimization.

Figure 8 indicates that a slight reduction in tube diameter to 0.0366 m would hinder performance, resulting in a 3%–5% decrease in both DME selectivity and productivity. Guffanti et al. (2021a) concluded that the overall DME yield—defined as amount of DME formed over amount of carbon supplied—decreases slightly in long-duration experiments when the tube diameter is increased. However, this trend is reversed when focusing on the region of maximum adsorption productivity, which is of particular interest. These findings are consistent with the results of the current study. The underlying mechanism for this effect is not entirely clear or confirmed. In addition to improved flow distribution and mass transfer, the observed reduction in DME yield may be attributed to the decreased reactor volume, which leads to an increase in Gas Hourly Space Velocity (GHSV). An elevated GHSV indicates a faster flow of gas through the reactor relative to the catalyst volume, which in turn reduces the residence time of gas-phase reactants on the catalyst surface, thereby limiting the conversion efficiency.

To investigate this hypothesis further, simulations with a tube diameter of 36.6 mm were conducted with a reduced volumetric flow rate of 18.57 Nm^3/h , corresponding to the same GHSV as in the 38 mm diameter simulation. This approach aims to isolate and quantify the effect of GHSV by ensuring comparable contact times for the gas-phase reactants across different tube diameters. As shown in Figure 8, this adjustment inevitably results in reduced productivity, due to lower reactant flow rate, but it preserves a similar range of DME selectivity. For reference, the maximum productivity for the 38 mm tube, it is 3.38 kg/h at 80.6% DME selectivity, while for the 36.6 mm tube is

3.14 kg/h at 80.9% DME selectivity. That shows that the dominant driver of the performance difference at different tube diameters is the GHSV.

It is concluded, that in the operating window of maximum DME productivity, larger tube diameters result in high DME productivities and higher carbon selectivity to DME. This effect is almost entirely attributed to the reduction of GHSV which enhances the contact of the reactants with the catalyst. At higher cycle durations outside the optimum productivity zone, where selectivity is further hindered, the performance at different tube diameters may be reverted due to temperature effects on chemical kinetics and water adsorption equilibria, as analysed by Guffanti et al. (2021a).

3.2.4 Effect of adsorption feed flow

Further analysis of Figure 8, comparing the two flow rates at a 36.6 mm tube diameter (20 and 18.7 Nm^3/h), provides valuable insights into the effect of feed flow rate in the SEDMES process. The graph clearly demonstrates that this slight reduction in flow results in a higher carbon selectivity to DME, which increases by approximately 4% when comparing same cycle durations. The maximum productivity point occurs at 80.9% DME selectivity compared to 77.6% at the higher flow rate. Although this improvement in selectivity is notable, it is not sufficient to offset the reduced reactant flow, leading to a decline in maximum achievable productivity from 3.24 kg/h to 3.14 kg/h, as expected.

Consistent with the findings in previous sections, the enhanced selectivity observed with the reduced flow rate is primarily attributed to the decrease in GHSV. The extended residence time allows for more efficient interaction between reactants and the catalyst, while also promoting the complete conversion of intermediates, such as methanol, into DME, as the reactants have adequate time to proceed through the desired reaction pathway. Additionally, as observed by van Kampen et al., the lower flow rate helps prevent water breakthrough and maintains the effectiveness of sorption enhancement throughout the adsorption step, further contributing to the improved selectivity (Van Kampen et al., 2020a).

4 Conclusion

For the first time, sorption enhanced DME synthesis (SEDMES) has been optimized by focusing on the key performance indicators of DME productivity and selectivity. The performance was analyzed under varying pressure levels, cycle durations, inert gas concentration, tube geometry and feed flow rates to quantify the trade-off between productivity and selectivity.

The results demonstrate that controlling any of these parameters—while keeping the others constant—leads to a peak in productivity, which is influenced by the rate of adsorbent saturation and water accumulation, depending on the input conditions. Cycle duration is the most significant parameter to control water adsorption and desorption, as it has no thermodynamic or significant economic limitation. By allowing cycle duration to remain as a free variable and selecting values that correspond to the maximum productivity, the study reveals a gradual diminishing increase in both productivity and selectivity with rising pressure. Maximum productivity increases from 2.2 kg/h with 50.2% DME selectivity at 20 bar to 3.6 kg/h with 88.5% DME selectivity at 50 bar. The optimal cycle duration for these points also increased from 113 to 233 min, respectively.

Despite the clear performance advantage of operating at elevated pressures during the adsorption step, the optimal pressure may not necessarily be the highest achievable. Results show that higher pressures lead to greater DME losses during the blowdown step, complicating the already existing trade-off between thermodynamic benefits and the operational costs and complexities associated with higher pressures. Ultimately, the optimal operating conditions will depend on the specific process requirements.

Additionally, the inclusion of inert gases was found to reduce the overall performance of the SEDMES process. This is due to both the lower reactant flow and the decreased efficiency of reactant-catalyst contact. However, simulations showed that SEDMES can tolerate a high level of inert gases (at least 50 wt % N₂) without significant detriment, potentially eliminating the need for certain pretreatment steps and offering economic savings. Furthermore, a lower Gas Hourly Space Velocity (GHSV), achieved either through an increase in tube diameter or a reduction in feed flow, leads to a notable improvement in carbon selectivity to DME by approximately 5%, despite a modest reduction of less than 7% in GHSV.

Data availability statement

The raw data supporting the conclusions of this article will be made available by the authors, without undue reservation.

Author contributions

IT: Writing—original draft, Writing—review and editing. AC: Writing—original draft, Writing—review and editing. GS: Writing—review and editing. SS: Writing—review and editing. JB: Writing—review and editing.

References

- Altinsoy, N. S., and Avci, A. K. (2024). Sorption enhanced DME synthesis by one-step CO₂ hydrogenation. *Chem. Eng. Process - Process Intensif.* 203 (April), 109874. doi:10.1016/j.cep.2024.109874
- Azizi, Z., Rezaeimanesh, M., Tohidian, T., and Rahimpour, M. R. (2014a). Dimethyl ether: a review of technologies and production challenges. *Chem. Eng. Process Intensif.* 82, 150–172. doi:10.1016/j.cep.2014.06.007
- Bercic, G., and Levec, J. (1992). Intrinsic and global reaction rate of methanol dehydration over gamma-alumina pellets. *Ind. Eng. Chem. Res.* 31 (4), 1035–1040. doi:10.1021/ie00004a010
- Boon, J. (2023). Sorption-enhanced reactions as enablers for CO₂ capture and utilisation. *Curr. Opin. Chem. Eng.* 40, 100919. doi:10.1016/j.coche.2023.100919
- Boon, J., Berkel, F. P. F., and Vente, J. F. (2017). Separation enhanced dimethyl ether synthesis. *Fifth Int Conf 2017 Tailor Made Fuels Biomass.*
- Boon, J., van Kampen, J., Hoogendoorn, R., Tanase, S., van Berkel, F. P. F., and van Sint, A. M. (2019). Reversible deactivation of γ -alumina by steam in the gas-phase dehydration of methanol to dimethyl ether. *Catal. Commun.* 119 (October 2018), 22–27. doi:10.1016/j.catcom.2018.10.008
- Borgschulte, A., Gallandat, N., Probst, B., Suter, R., Callini, E., Ferri, D., et al. (2013). Sorption enhanced CO₂ methanation. *Phys. Chem. Chem. Phys.* 15 (24), 9620–9625. doi:10.1039/c3cp51408k
- Catizzone, E., Bonura, G., Migliori, M., Frusteri, F., and Giordano, G. (2017). CO₂ recycling to dimethyl ether: state-of-the-art and perspectives. *Molecules* 23 (1), 31–28. doi:10.3390/molecules23010031
- Catizzone, E., Freda, C., Braccio, G., Frusteri, F., and Bonura, G. (2021). Dimethyl ether as circular hydrogen carrier: catalytic aspects of hydrogenation/dehydrogenation steps. *J. Energy Chem.* 58, 55–77. Science Press. doi:10.1016/j.jechem.2020.09.040
- Dadgar, F., Myrstad, R., Pfeifer, P., Holmen, A., and Venvik, H. J. (2016). Direct dimethyl ether synthesis from synthesis gas: the influence of methanol dehydration on methanol synthesis reaction. *Catal. Today* 270, 76–84. doi:10.1016/j.cattod.2015.09.024
- De Falco, M., Capocelli, M., and Basile, A. (2017). Selective membrane application for the industrial one-step DME production process fed by CO₂ rich streams: modeling and simulation. *Int. J. Hydrogen Energy* 42 (10), 6771–6786. doi:10.1016/j.ijhydene.2017.02.047
- Delbeke, J., Runge-Metzger, A., Slingenberg, Y., and Werksman, J. (2019). The paris agreement. *Towar. a Clim. Eur. Curbing Trend.*, 24–45. doi:10.4324/9789276082569-2
- Dieterich, V., Buttler, A., Hanel, A., Spliethoff, H., and Fendt, S. (2020). Power-to-liquid via synthesis of methanol, DME or Fischer–Tropsch-fuels: a review. *Energy Environ. Sci.* 13 (10), 3207–3252. doi:10.1039/d0ee01187h
- Elsner, M. P., Dittrich, C., and Agar, D. W. (2002). Adsorptive reactors for enhancing equilibrium gas-phase reactions—two case studies. *Chem. Eng. Sci.* 57 (9), 1607–1619. doi:10.1016/s0009-2509(02)00037-4
- Elsner, M. P., Menge, M., Müller, C., and Agar, D. W. (2003). The Claus process: teaching an old dog new tricks. *Catal. Today* 79–80, 487–494. doi:10.1016/s0920-5861(03)00071-3
- European Commission (2019). The European green deal. Commun from com to eur parliament. *Counc. Eur. Econ. Soc. committee Comm. Reg.* 35, 44–67. Available at: <https://eur-lex.europa.eu/legal-content/EN/TXT/?uri=COM%3A2019%3A640%3AFIN>.
- European Commission (2021). European climate law. *Off. J. Eur. Union* 2021 (June), 17. Available at: <https://eur-lex.europa.eu/legal-content/EN/TXT/?uri=CELEX:32021R1119>.
- Gabruš, E., Nastaj, J., Tabero, P., and Aleksandrak, T. (2015). Experimental studies on 3A and 4A zeolite molecular sieves regeneration in TSA process: aliphatic alcohols dewatering-water desorption. *Chem. Eng. J.* 259, 232–242. doi:10.1016/j.cej.2014.07.108

Funding

The author(s) declare that financial support was received for the research, authorship, and/or publication of this article. The work in this publication was performed with a subsidy from the Ministry of Economic Affairs and Climate and the Ministry of Agriculture, Nature and Food Quality, National EZK and LNV subsidy schemes, Top Sector Energy implemented by the Netherlands Enterprise Agency (RVO).

Conflict of interest

The authors declare that the research was conducted in the absence of any commercial or financial relationships that could be construed as a potential conflict of interest.

The author(s) declared that they were an editorial board member of *Frontiers*, at the time of submission. This had no impact on the peer review process and the final decision.

Generative AI statement

The author(s) declare that no Generative AI was used in the creation of this manuscript.

Publisher's note

All claims expressed in this article are solely those of the authors and do not necessarily represent those of their affiliated organizations, or those of the publisher, the editors and the reviewers. Any product that may be evaluated in this article, or claim that may be made by its manufacturer, is not guaranteed or endorsed by the publisher.

- Graaf, G. H., Stamhuis, E. J., and Beenackers, AACM (1988). Kinetics of low-pressure methanol synthesis. *Chem. Eng. Sci.* 43 (12), 3185–3195. doi:10.1016/0009-2509(88)85127-3
- Guffanti, S., Visconti, C. G., and Groppi, G. (2021c). Model analysis of the role of kinetics, adsorption capacity, and heat and mass transfer effects in sorption enhanced dimethyl ether synthesis. *Ind. Eng. Chem. Res.* 60 (18), 6767–6783. doi:10.1021/acs.iecr.1c00521
- Guffanti, S., Visconti, C. G., van Kampen, J., Boon, J., and Groppi, G. (2021a). Reactor modelling and design for sorption enhanced dimethyl ether synthesis. *Chem. Eng. J.* 404, 126573. doi:10.1016/j.cej.2020.126573
- Iliuta, I., Iliuta, M. C., and Larachi, F. (2011). Sorption-enhanced dimethyl ether synthesis-Multiscale reactor modeling. *Chem. Eng. Sci.* 66 (10), 2241–2251. doi:10.1016/j.ces.2011.02.047
- Jia, Le N., and Yin, F. Y. (2024). Catalytic conversion of CO₂ to dimethyl ether: a review of recent advances in catalysts and water selective layer. *J. Ind. Eng. Chem.* 140, 88–102. doi:10.1016/j.jiec.2024.05.058
- Kampen, J. V., Boon, J., Berkel, F. P. F., Dijk, H. A. J., Vente, J. F., and Annaland, M. V. S. (2018). Regeneration conditions as the key to sorption enhanced dimethyl ether synthesis. *25th Int. Conf. Chem. React. Eng.* 1, 3–4.
- Kim, H. J., Jung, H., and Lee, K. Y. (2001). Effect of water on liquid phase DME synthesis from syngas over hybrid catalysts composed of Cu/ZnO/Al₂O₃ and γ -Al₂O₃. *Korean J. Chem. Eng.* 18 (6), 838–841. doi:10.1007/bf02705605
- Kim, K. M., Oh, H. T., Lim, S. J., Ho, K., Park, Y., and Lee, C. H. (2016). Adsorption equilibria of water vapor on zeolite 3A, zeolite 13X, and dealuminated Y zeolite. *J. Chem. Eng. Data* 61 (4), 1547–1554. doi:10.1021/acs.jced.5b00927
- Liuzzi, D., Peinado, C., Peña, M. A., Van Kampen, J., Boon, J., and Rojas, S. (2020). Increasing dimethyl ether production from biomass-derived syngas: via sorption enhanced dimethyl ether synthesis. *Sustain Energy Fuels* 4 (11), 5674–5681. doi:10.1039/d0se01172j
- Merkouri, L. P., Ahmet, H., Ramirez Reina, T., and Duyar, M. S. (2022). The direct synthesis of dimethyl ether (DME) from landfill gas: a techno-economic investigation. *Fuel* 319, 123741. doi:10.1016/j.fuel.2022.123741
- Mohamud, M. Y., Abdullah, T. A. T., Ahmad, A., Ikram, M., Alir, A., Phey, M. L. P., et al. (2023). Direct synthesis of dimethyl ether from CO₂ hydrogenation over core-shell nanotube Bi-functional catalyst. *Catalysts* 13 (2), 408–418. doi:10.3390/catal13020408
- Nimmas, T., Wongsakulphasatch, S., Chanthanumataporn, M., Vacharanukrauh, T., and Assabumrungrat, S. (2024). Thermochemical transformation of CO₂ into high-value products. *Curr. Opin. Green Sustain Chem.* 47 (1), 100911. doi:10.1016/j.cogsc.2024.100911
- Peinado, C., Liuzzi, D., Sluijter, S. N., Skorikova, G., Boon, J., Guffanti, S., et al. (2024). Review and perspective: next generation DME synthesis technologies for the energy transition. *Chem. Eng. J.* 479 (August 2023), 147494. doi:10.1016/j.cej.2023.147494
- Saravanan, K., Ham, H., Tsubaki, N., and Bae, J. W. (2017). Recent progress for direct synthesis of dimethyl ether from syngas on the heterogeneous bifunctional hybrid catalysts. *Appl. Catal. B Environ.* 217, 494–522. doi:10.1016/j.apcatb.2017.05.085
- Schmidt-Traub, H., and Górák, A. (2006). Integrated reaction and separation operations: modelling and experimental validation. *Integr. React. Sep. Oper. Model Exp. Valid.*, 1–366.
- Skorikova, G., Saric, M., Sluijter, S. N., van Kampen, J., Sánchez-Martínez, C., and Boon, J. (2020). The techno-economic benefit of sorption enhancement: evaluation of sorption-enhanced dimethyl ether synthesis for CO₂ utilization. *Front. Chem. Eng.* 2. doi:10.3389/fceng.2020.594884
- Styring, P., Sanderson, P. W., Gell, I., Skorikova, G., Sánchez-Martínez, C., Garcia-Garcia, G., et al. (2022). Carbon footprint of Power-to-X derived dimethyl ether using the sorption enhanced DME synthesis process. *Front. Sustain* 3 (Red II). doi:10.3389/frsus.2022.1057190
- van Kampen, J., Boon, J., van Berkel, F., Vente, J., and van Sint Annaland, M. (2019a). Steam separation enhanced reactions: review and outlook. *Chem. Eng. J.* 374, 1286–1303. doi:10.1016/j.cej.2019.06.031
- van Kampen, J., Boon, J., Vente, J., and Van Sint Annaland, M. (2020a). Sorption enhanced dimethyl ether synthesis for high efficiency carbon conversion: modelling and cycle design. *J. CO₂ Util.* 37 (October 2019), 295–308. doi:10.1016/j.jcou.2019.12.021
- van Kampen, J., Boon, J., Vente, J., and Van Sint Annaland, M. (2021). Sorption enhanced dimethyl ether synthesis under industrially relevant conditions: experimental validation of pressure swing regeneration. *React. Chem. Eng.* 6 (2), 244–257. doi:10.1039/d0re00431f
- van Kampen, J., Booneveld, S., Boon, J., Vente, J., and Van Sint, A. M. (2020b). Experimental validation of pressure swing regeneration for faster cycling in sorption enhanced dimethyl ether synthesis. *Chem. Commun.* 56 (88), 13540–13542. doi:10.1039/d0cc06093c
- van Kampen, J., Overbeek, J., Boon, J., and van Sint Annaland, M. (2023). Continuous multi-column sorption-enhanced dimethyl ether synthesis (SEDMES): dynamic operation. *Front. Chem. Eng.* 5 (February), 1–10. doi:10.3389/fceng.2023.1055896
- van Vuuren, D. P., Boot, P. A., Ros, J., Hof, A. F., and den Elzen, M. G. (2017). The implications of the Paris climate agreement for the Dutch climate policy objectives. *PBL Neth. Environ. Assessment Agency* (October), 1–29. Available at: <http://www.pbl.nl/sites/default/files/cms/publicaties>.
- Walspurger, S., Elzinga, G. D., Dijkstra, J. W., Sarić, M., and Haije, W. G. (2014). Sorption enhanced methanation for substitute natural gas production: experimental results and thermodynamic considerations. *Chem. Eng. J.* 242, 379–386. doi:10.1016/j.cej.2013.12.045

